Available online at www.sciencedirect.com
ScienceDirect
Journal of Nuclear Materials 363–365 (2007) 633–637
journal of nuclear materials
www.elsevier.com/locate/jnucmat

Numerical predictions of the poloidal $E \times B$ drift in EAST

J. Ou *, S. Zhu

Institute of Plasma Physics, Chinese Academy of Sciences, Hefei 230031, China

Abstract

The effects of poloidal $E \times B$ drift in EAST are study with a one-dimensional fluid code. The transport equations are solved in the poloidal direction with the radial particle and energy influxes as source terms. The simulation results show that the effects of poloidal $E \times B$ drift on the plasma density and temperature are stronger in high recycling case than in detached case. With the core-edge density increasing, the tendency of $p^{\text{outer}}/p^{\text{inner}}$ is to decrease for normal B_T and to increase for reversed B_T. The ratios of the outer/inner particle and energy fluxes increase with P_{SOL} for normal B_T and decrease with reversed B_T. The degree of divertor asymmetries due to the poloidal $E \times B$ drift is reduced at low power and high density for both normal and reversed B_T, as expected.

PACS: 52.25.Fi

Keywords: Divertor plasma; Divertor modeling; Particle drift; EAST

1. Introduction

In/out divertor asymmetry has been observed experimentally in several tokamaks with a single-null divertor configuration [1–3]. Moreover, the degree of in/out divertor asymmetries depends on the line averaged density [1,2]. The outer/inner divertor energy asymmetry increases with the heating power from the core plasma for normal toroidal field and decreases with reversed toroidal field [3]. When the detachment occurs, the asymmetry in the poloidal flux is small compared to that in the attached divertor [4]. To analyze these experimental phenomena, which also could be observed in coming experiment in EAST, a one-dimensional fluid model including the poloidal $E \times B$ drift presented in Ref. [5] was used. In this paper, we improve the model and apply it to investigate the effect of the poloidal $E \times B$ drift in high recycling case and detached case of the OH-L plasma experiments for EAST.

2. Simulation model

We apply the 1-D model including the poloidal $E \times B$ drift based on the 2-D fluid transport equations [6], assuming that ion and electron temperatures are equal, and that density and temperature both decay exponentially in the radial direction with the e-folding length λ_n and λ_T. Then, a

* Corresponding author. Tel.: +86 551 559 3184; fax: +86 551 559 1310.
E-mail address: ouj@ipp.ac.cn (J. Ou).

0022-3115/$ - see front matter © 2007 Elsevier B.V. All rights reserved.
doi:10.1016/j.jnucmat.2007.01.070

one-dimensional model is applied in the poloidal direction with the radial influxes of the particles and energy as source terms. This model uses a simplified geometry and the charge neutrality. Viscosity is not taken into account and currents are also neglected.

The poloidal $E\times B$ drift velocity enters the transport equations through the poloidal velocity:

$$V_\theta = \frac{B_\theta}{B}V_\parallel + V_\theta^{\text{drift}}. \tag{1}$$

The poloidal $E\times B$ drift can be estimated from [5]

$$V_\theta^{\text{drift}} = \frac{3.0KT}{e\lambda_T B}. \tag{2}$$

The equations for particle conservation and energy can be written as

$$\frac{\partial}{\partial\theta}(nV_\theta) = S_{\text{p}}, \tag{3}$$

$$\frac{\partial}{\partial\theta}\left(5nV_\theta T - \left(\frac{B_\theta}{B}\right)^2\kappa_{\text{e}}\frac{\partial T}{\partial\theta}\right) = S_{\text{n}}. \tag{4}$$

The radial derivative of the particle flux Γ_{r} and energy Q_{r} are replaced by the e-folding length λ_n and λ_T

$$\frac{\partial}{\partial r}\Gamma_{\text{r}} = \frac{\partial}{\partial r}nV_{\text{r}} = \frac{\partial}{\partial r}\frac{D}{\lambda_n}n = -\frac{D}{\lambda_n^2}n, \tag{5}$$

$$\begin{aligned}\frac{\partial}{\partial r}Q_{\text{r}} &= \frac{\partial}{\partial r}\left(5\Gamma_{\text{r}}T - 2\kappa_{\text{r}}\frac{\partial T}{\partial r}\right)\\ &= -\left(\frac{1}{\lambda_n}+\frac{1}{\lambda_T}\right)Q_{\text{r}} = -\left(\frac{1}{\lambda_n}+\frac{1}{\lambda_T}\right)\left(5\frac{D}{\lambda_n}+\frac{2\chi_{\text{r}}}{\lambda_T}\right)nT.\end{aligned} \tag{6}$$

The sources terms:

$$S_{\text{p}} = -\frac{\partial}{\partial r}\Gamma_{\text{r}} + nn_{\text{n}}\langle\sigma v\rangle_{\text{sion}}, \tag{7}$$

$$S_{\text{n}} = -\frac{\partial}{\partial r}Q_{\text{r}} + \varepsilon_{\text{ion}}nn_{\text{n}}\langle\sigma v\rangle_{\text{sion}} - W_{\text{imp}} - \frac{3}{2}Tnn_{\text{n}}\langle\sigma v\rangle_{\text{cex}}. \tag{8}$$

The second term on the right-hand side of expression in (8) is the energy loss due to the ionization and excitation ($\varepsilon_{\text{ion}} = -20.0$ eV). The term W_{imp} is the radiation-cooling rate of impurity ions. The last is due to charge exchange.

Here, the radial term in the momentum equation is omitted, so the equation for momentum looks as follows:

$$\frac{\partial}{\partial\theta}\left(mnV_\parallel V_\theta + 2\frac{B_\theta}{B}nT\right) = S_{\text{m}}. \tag{9}$$

The momentum source is defined as:

$$S_{\text{m}} = -mV_\parallel nn_{\text{n}}\langle\sigma v\rangle_{\text{cex}}. \tag{10}$$

The boundary conditions at the two divertors for the poloidal velocity and the poloidal heat fluxes are

$$V_{\theta|d} = \pm\frac{B_\theta}{B}c_{\text{s}}, \tag{11}$$

$$Q_{\theta|d} = \pm\gamma\frac{B_\theta}{B}c_{\text{s}}n_{\text{d}}T_{\text{d}}. \tag{12}$$

Here, we have imposed the Bohm condition for the plasma velocity at the divertor target. γ is the sheath energy transmission factor. If no secondary emission at the target is considered for the hydrogen plasma with $T_i = T_e$, the factor is approximately 5.5.

The neutral gas model assumes that the neutrals emitted from the divertor are diffusing across the background plasma through charge exchange process. The diffusion equation for neutral density is given by

$$-\frac{\partial}{\partial\theta}\left(D_{\text{n}}\frac{\partial n_{\text{n}}}{\partial\theta}\right) = -nn_{\text{n}}\langle\sigma v\rangle_{\text{sion}}. \tag{13}$$

The diffusion coefficient D_{n} due to the charge exchange is

$$D_{\text{n}} = \frac{T}{m_i n\langle\sigma v\rangle_{\text{cex}}}. \tag{14}$$

For the neutral gas recycled from incident ions on the divertor plates, the poloidal particle flux is specified as a fraction R_{SOL} of the incident ion flux, i.e.,

$$\left(D_{\text{n}}\frac{\partial n_{\text{n}}}{\partial\theta}\right)_{|d} = R_{\text{SOL}}nV_{\theta|d}. \tag{15}$$

The impurity radiation W_{imp} is given by

$$W_{\text{imp}} = nn_{\text{I}}L(T), \tag{16}$$

where n_{I} is the density of impurity ions, $L(T)$ is the impurity cooling rate and only depends on the plasma temperature [7]. Carbon is the only impurity species considered in our simulations. The density n_{I} is given by using a fixed fraction model

$$n_{\text{I}} = \xi n, \tag{17}$$

where, the constant ξ is the impurity fraction.

3. Simulation results and discussion

To study the effect of poloidal $E\times B$ drift in EAST, we perform calculations for a parameter

set of L-mode operation. The main parameters of EAST for modeling are listed in Table 1 [8,9].

The heating power P_{SOL}, assumed to be uniform on the separatrix, escaping from the core plasma, are defined by $P_{SOL} = Q_r \cdot S_{sep}$, where the S_{sep} is the separatrix surface area. The temperature decay length λ_T and the density decay length λ_n are important lengths in the model. Since EAST SOL performance for these two lengths cannot yet be reliably predicted from theory, temperature decay length λ_T can be based on the characteristics of present tokamaks. As an example, in high temperature regime, i.e $T_{e-sep} > 40$–50 eV, for the OH-L plasma, in which λ_T varies only moderately, λ_T may be brought into order by the relationship [10]

$$\lambda_T(m) = 112R(\mathrm{mag})^{1.21\pm0.04} I_p(A)^{-0.69\pm0.03}. \quad (18)$$

So, the λ_n can be obtained from the Eq. (6) at the stagnation point when we give values of input power and edge-core density.

$$Q_r = \left(\frac{5D}{\lambda_n} + \frac{2\chi_r}{\lambda_T}\right) n_0 T_0. \quad (19)$$

High recycling plasma and detached plasma are the two typical divertor-plasma regimes. In high recycling case, the pressure is conserved on a field line and losses of the momentum and power are small. Most of the power actually deposit on the target. Compared with high recycling case, detached case clearly involves large pressure gradients along the magnetic field with quite low plasma power to the targets. With the parameters listed in Table 2, the effects of poloidal $E \times B$ drift in high recycling and detached regimes can be discussed.

The poloidal profiles of the ratios of plasma temperature and density with drift on/off are shown in Fig. 1. In the high recycling case, we can see that poloidal $E \times B$ drift clearly influences the plasma density and temperature, especially in the recycling zone. In the vicinity of the outer target, the ratio of the density with and without poloidal $E \times B$ drift is up to 1.25 for the normal field (ion ∇B drift is directed toward the X-point), while for the reversed field (ion ∇B drift is directed away from the X-point), the ratio is less than 0.86. The influence by the poloidal $E \times B$ drift on the temperature is less than that on the density. In the detached case, the ratio of the density with and without poloidal $E \times B$ drift is less than 1.1 for the normal field near the outer target, while for the reversed field, the ratio is larger than 0.90. For both normal and reversed field, the ratio of the temperature with and without poloidal $E \times B$ drift shows a very slight changes near the 1.0. In other words, the effects of the $E \times B$ drift are also observed in the detached case in the simulations, but the effect on the plasma density and temperature is shown to be relatively small. This is similar to the numerical results in JT-60U [11].

The degree of in/out density and temperature asymmetry can change dramatically with the line averaged density. For example in Alcator C-Mod and ASDEX-Upgrade, the asymmetry of

Table 1
The main parameters of EAST

Major radius R (m)	1.97
Minor radius a (m)	0.5
Elongation κ	1.6–2.0
Toroidal field B_0 (T)	3.5
Plasma current I_P (MA)	1.0
Particle diffusivity D (m^2/s)	0.5–1.0
Radial thermal diffusivity χ_r (m^2/s)	1.0–2.0
Impurity fraction (carbon) ξ	0.05

Table 2
Parameters of plasmas for high recycling and detached case

	High recycling	Detached
$n^{core-edge}$ (10^{19} m^{-3})	1.5	2.5
P_{SOL} (MW)	1.37	0.85
R_{SOL}	0.95	0.98

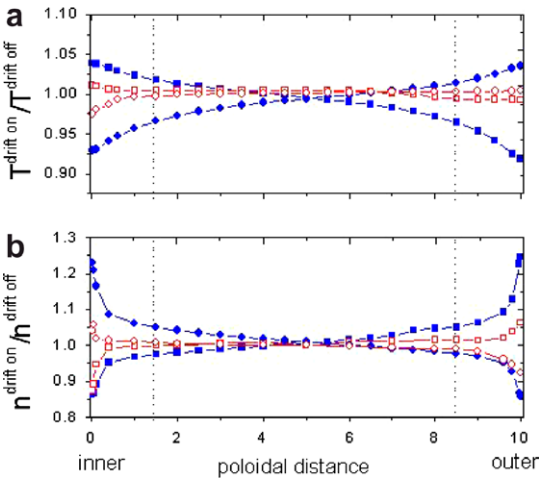

Fig. 1. Ratios of plasma temperature and density with the poloidal $E \times B$ drift on/off as a function of the poloidal distance for the following cases: (■)-normal field, attached case; (●)-reversed field, attached case; (□)-normal field, detached case; (○)-reversed field, detached case.

temperature is large at low densities and decreases at high densities [1,2]. To investigate the degree of out/in asymmetries of density, temperature and pressure as a function of line averaged density, we have carried out a series of simulations with varying the core-edge densities. Fig. 2 shows that the out/in density and temperature asymmetries depend on the core-edge density. With the core-edge density increasing, $n^{\text{outer}}/n^{\text{inner}}$ tends to increase while $T^{\text{outer}}/T^{\text{inner}}$ tends to decrease for the normal toroidal field. When the field is reversed, the tendencies of the asymmetry ratios reverse. For the out/in pressure asymmetry, $p^{\text{outer}}/p^{\text{inner}} > 1$ and the ratio decreases with core edge density increasing for the normal toroidal field, while $p^{\text{outer}}/p^{\text{inner}} < 1$ and the ratio increases. The out/in asymmetry associated with the poloidal $E \times B$ drift can be written as [12]

$$\frac{p^{\text{outer}}}{p^{\text{inner}}} \approx \frac{2 - M_{\text{E,in}}}{2 + M_{\text{E,out}}}.$$

M_{E} is Mach number which is negative with normal toroidal field and positive with the toroidal field reversal. Since the static pressure tends to reach equilibrium along the field lines, when the core-edge density increases, the temperature decreases. According to Eq. (2), the poloidal $E \times B$ drift becomes small and the tendency of $p^{\text{outer}}/p^{\text{inner}}$ approaches to 1.0.

Fig. 3 shows that the out/in ratios of particle flux $\Gamma^{\text{outer}}/\Gamma^{\text{inner}}$ and energy flux $E^{\text{outer}}/E^{\text{inner}}$ as a function of the heating power P_{SOL}. The simulation shows that the divertor asymmetries obviously

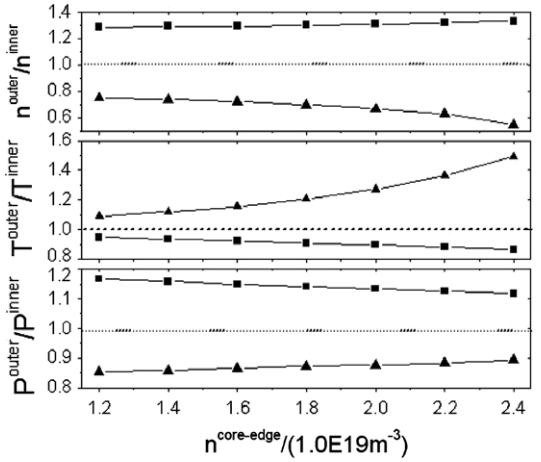

Fig. 2. Ratios of out/in density, temperature and pressure as a function of core-edge density with heat power $P_{\text{SOL}} = 1.10$ MW and recycling coefficient $R_{\text{SOL}} = 0.93$: (■)-normal field; (▲)-reversed field.

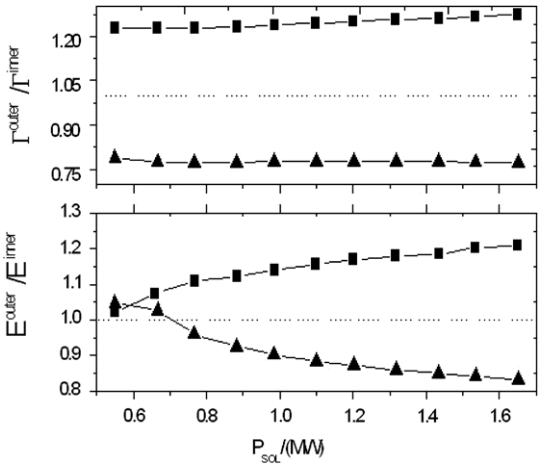

Fig. 3. Ratios of out/in particle flux and energy flux as a function of the heating power from the core plasma P_{SOL} with core-edge density $n^{\text{core-edge}} = 2.0 \times 10^{19}\ \text{m}^{-3}$ and recycling coefficient $R_{\text{SOL}} = 0.90$: (■)-normal field; (▲)-reversed field.

depend on the direction of the toroidal field. It appears that ratios of both $\Gamma^{\text{outer}}/\Gamma^{\text{inner}}$ and $E^{\text{outer}}/E^{\text{inner}}$ increase with P_{SOL} for normal toroidal field and decrease with P_{SOL} for reversed toroidal field. Thus, the effect of the poloidal $E \times B$ drift on the particle flux and the energy flux must be larger a higher P_{SOL} than that at low P_{SOL}. It is interesting to note that $E^{\text{outer}}/E^{\text{inner}}$ appears to be strongly dependent on the heating power for both normal and reversal toroidal field, showing the same tendency as observed in JET [3].

The effect of poloidal $E \times B$ drift may be seen by comparing the ratio of poloidal $E \times B$ drift flux to the poloidal flux caused by the parallel sonic flow. If the difference between ion and electron temperatures is ignored, poloidal fluxes for $E \times B$ drifts can be estimated as

$$\Gamma_\theta^{\text{dr}} = \frac{3kTn}{e\lambda_T B}. \tag{20}$$

Parallel flow with the sound speed causes poloidal flux

$$\Gamma_\theta^{\parallel} \approx nc_s B_\theta / B. \tag{21}$$

The ratio of the two fluxes can be expressed as

$$\Gamma_\theta^{\text{dr}} / \Gamma_\theta^{\parallel} \approx \rho_{s\theta}/\lambda_T, \tag{22}$$

where, $\rho_{s\theta} \equiv c_s/\omega_{i\theta}$ and $\omega_{i\theta} = eB_\theta/m_i$, the ion poloidal gyro-frequency.

With the Eq. (18), the dependence of the ratio of the two fluxes on temperature T is

$$\Gamma_\theta^{dr}/\Gamma_\theta^{\parallel} \propto T^{1/2}. \quad (23)$$

It follows from Eq. (23) that the polodial $E \times B$ drift should play a relatively small role in low-power heated, high-density discharges, which have low temperature throughout the SOL and divertor, consistent with the numerical results.

Note that our present model can only make some qualitative predictions. It is difficult to predict actual divertor asymmetries. In particular, it is still unclear what determines the divertor asymmetry. For single-null divertor operation, it has been observed that the power flux to the outer target is usually much higher than that to the inner target, typically $E^{outer}/E^{inner} \sim 2$ or higher for normal toroidal field, which cannot be simply attributed to the poloidal $E \times B$ drift [12]. According to the analysis performed in [13], the poloidal $E \times B$ drifts were dominated over by the radial $E \times B$ drifts in high recycling plasma. In our model, we solved only transport equations in the poloidal direction, and the radial $E \times B$ drifts are not included in the present analysis.

4. Conclusion and future study

To investigate the effects of poloidal $E \times B$ drift in high recycling case and detached case of the OH-L plasma experiments for EAST, a simplified fluid model has been developed. In this model, we solved transport equations in the poloidal direction, with the radial fluxes of the particle and energy as source terms.

With this model, we have shown that the poloidal $E \times B$ drift influences the plasma transport in the simulation. In the high recycling regime, the poloidal $E \times B$ drift clearly influences the density and temperature asymmetries. While in the detached regime, the effects of the poloidal $E \times B$ drift on the poloidal profiles of density and temperature are very small. With the core-edge density increasing, the ratios of the out/in pressure p^{outer}/p^{inner} and temperature T^{outer}/T^{inner} tend to decrease for normal toroidal field and to increase for reversed toroidal field. But the ratio of the density n^{outer}/n^{inner} tends to increase for normal toroidal field and to decrease for reversed toroidal field. As the heating power increases, the ratios of the out/in particle and energy fluxes, $\Gamma^{outer}/\Gamma^{inner}$, E^{outer}/E^{inner}, both increase with P_{SOL} for normal toroidal field and decrease with P_{SOL} for reversed toroidal field with a more pronounced change in energy fluxes. The numerical modeling shows that the poloidal $E \times B$ drift has a stronger effect on high-power heated, low-density plasma, as the poloidal flux due to the $E \times B$ drift to that caused by the parallel sonic flow scales as $T^{1/2}$.

The one-dimension fluid model is shown to be useful for understanding the effect of poloidal $E \times B$ drift in EAST. To further investigate the divertor asymmetry, the radial $E \times B$ drift will be taken into account. In addition, two-dimensional simulation of the SOL and divertor plasmas including various $E \times B$ and diamagnetic drifts will be carried out in the future study.

References

[1] I.H. Hutchinson et al., Plasma Phys. Control. Fus. 37 (1995) 1389.
[2] N. Tsois et al., J. Nucl. Mater. 266–269 (1999) 1230.
[3] R.A. Pitts et al., J. Nucl. Mater. 337–339 (2005) 146.
[4] N. Asakura et al., Nucl. Fusion 44 (2004) 503.
[5] M. Lehnen et al., Nucl. Fusion 43 (2003) 168.
[6] M. Baelmans, KFA-Report, JVL-2891 and LPP-ERM/KMS-Rep NO 100, 1994.
[7] J. Wesson, Tokamaks Published in the US by Oxford University, Inc., New York, 1997, p. 209.
[8] W. Yuanxi et al., Nucl. Fusion 40 (2000) 1057.
[9] S. Zhu, X. Zha, J. Nucl. Mater. 313–316 (2003) 1020.
[10] ITER Physicis Expert Group on Divertor, Nucl. Fusion. 39 (1999) 2391.
[11] K. Hoshino et al., J. Nucl. Mater. 337–339 (2005) 276.
[12] A.V. Chankin, J. Nucl. Mater. 241–243 (1997) 199.
[13] P.C. Stangeby, A.V. Chankin, Nucl. Fusion 36 (1996) 839.